Macromolecules

ARTICLE

pubs.acs.org/Macromolecules

# Isoselectivity and Steric Hindrance of $C_2$ Symmetric Metallocenes as the Keys to Control Structural and Thermal Features of Ethene/4-Methyl-1-Pentene Copolymers

Paola Stagnaro,[*,†] Luca Boragno,[†] Simona Losio,[*,‡] Maurizio Canetti,[‡] Giovanni Carlo Alfonso,[§] Maurizio Galimberti,[⊥] Fabrizio Piemontesi,[∥] and Maria Carmela Sacchi[‡]

[†]ISMAC—Genova, Istituto per lo Studio delle Macromolecole ISMAC—CNR, Via De Marini 6, 16149 Genova, Italy

[‡]ISMAC—Milano, Istituto per lo Studio delle Macromolecole ISMAC—CNR, Via Bassini 15, 20133 Milano, Italy

[§]Dipartimento di Chimica e Chimica Industriale DCCI, Università di Genova, Via Dodecaneso 31, 16146 Genova, Italy

[⊥]Dipartimento di Chimica, Materiali e Ingegneria Chimica G. Natta, Politecnico di Milano, Via Mancinelli 7, 20131 Milano, Italy

[∥]Basell Poliolefine Italia Srl, P.le Donegani 12, 44122 Ferrara, Italy

Supporting Information

**ABSTRACT:** This work presents novel and, to some extent, surprising information on ethene/4-methyl-1-pentene (E/Y) copolymers prepared with $C_2$ symmetric single center metallocene catalysts: the moderately isopecific *rac*-ethylenebis(tetrahydroindenyl)zirconium dichloride (**EBTHI**) and the highly isospecific *rac*-dimethylsilylbis(2-methyl-4-phenylindenyl)zirconium dichloride (**MPHI**). *Blocky* E/Y copolymers from **EBTHI**, with relatively long sequences of both comonomers, underwent a thorough structural and thermal characterization, performed by combining WAXD, DSC and SSA thermal fractionation. The presence of crystallinities arising from both comonomers, as a function of the copolymer composition led to figure out the simultaneous presence of two populations of thin and defective crystals due to sequences of both comonomers, in samples with almost equimolar composition. The most isospecific metallocene, **MPHI**, was used exactly with the aim of finally preparing block E/Y copolymers, with long crystalline sequences of both comonomers, whose simultaneous presence could be clearly detected. The easiest 1-olefin propagation ever observed in E/Y copolymerization was obtained with **MPHI**. However, surprisingly, short sequences of Y were detected in the presence of short E sequences as well. Chain generation, performed for copolymers from both **EBTHI** and **MPHI**, revealed, in the latter case, a novel and unique microstructure, with very short sequences of both comonomers almost randomly distributed along the polymer chain. An amorphous nature of these copolymers was revealed by thermal analysis. This paper proposes thus an apparent paradox: on one side, it is confirmed that the 1-olefin propagation becomes easier by increasing the catalyst isoselectivity and, on the other side, short 1-olefin sequences are formed with the most isospecific metallocene. A way to come out from this *impasse* is proposed, taking into consideration the low steric hindrance of the most isospecific metallocene and the consequent higher reactivity for the 1-olefin, that leads to a lower concentration of 1-olefin in the polymerization bath and of 1-olefin sequences in the copolymer chain. For the first time it seems possible to tell apart the influence of isoselectivity and steric hindrance of a single center $C_2$ symmetric catalyst on structure and properties of ethene/1-olefin copolymers. This work reveals the existence of unexpected degrees of freedom for tuning micro- and macro-structures of ethene/1-olefin copolymers from $C_2$ symmetric metallocenes and wants to be a contribution for developing polymerizations able to control the monomer sequences, proposed as the Holy Grail in polymer science.

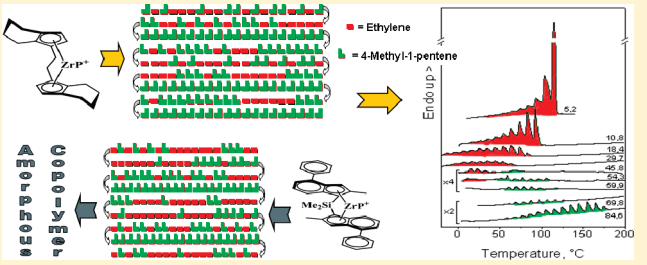


## INTRODUCTION

In the early days of ethene/1-olefin copolymerizations promoted by single center metallocene-based catalysts, it was proposed the correlation between metallocene symmetry and comonomer distribution along the polymer chain.[1] Upon comparing the behavior in ethene/propene copolymerization of aspecific $C_{2v}$, isospecific $C_2$, and syndiospecific $C_s$ organometallic complexes, it was reported that "the nonbonded interactions of the incoming monomer with some carbon atoms of the growing chain" were responsible of the relative comonomer reactivity and it was also hypothesized that the considered *some carbon atoms* could not protrude toward the incoming monomer when a metallocene had a $C_2$ symmetry. Moving from this intuition, research activity was performed over the elapsed years, that led to

**Received:** March 24, 2010
**Revised:** April 4, 2011
**Published:** April 26, 2011

**Chart 1. Isoselective $C_2$ Symmetric Metallocenes: (a) [*rac*-(EBTHI)$ZrCl_2$]; (b) [*rac*-$Me_2Si$(2-Me-4-PhInd)$_2ZrCl_2$]**

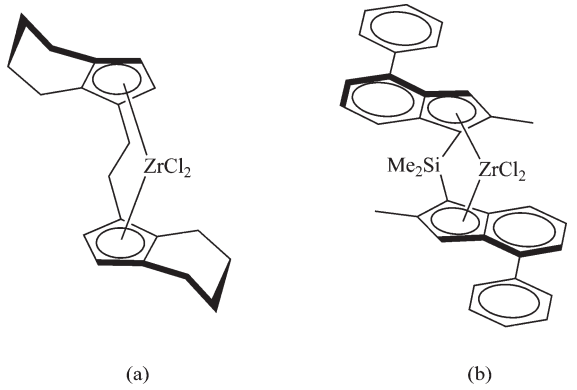


establish that a $C_2$ symmetric highly isospecific metallocene, having a remarkable steric hindrance, is able to promote an ethene/propene copolymerization characterized by a high $r_1r_2$ product of reactivity ratios, unusually arising from relatively high values of both $r_1$ and $r_2$. The use of a comonomer bulkier than propene, such as 4-methyl-1-pentene, led then to apply, for the first time to an insertion copolymerization, the concept that the enantioselectivity of a catalytic center is given by the cooperation of the intrinsic chirality of the organometallic complex and of the consequent placement of the growing chain. In fact, the bulkiness of 4-methyl-1-pentene as comonomer unit in the polymer chain was able to cause the upsurge of the catalyst stereoselectivity and ethene/4-methyl-1-pentene copolymers with relatively long sequences of both comonomers were prepared also from moderately isopecific metallocenes, such as *rac*-ethylenebis(indenyl)zirconium dichloride [*rac*-(EBI)$ZrCl_2$] (**EBI**) and *rac*-ethylenebis(tetrahydroindenyl)zirconium dichloride [*rac*-(EBTHI)$ZrCl_2$] (**EBTHI**).[2]

The high isoselectivity and the steric hindrance were thus shown to be the key features of non living single center catalysts for the preparation of *blocky* copolymers, allowing an easy propagation not only of ethene, but also of the 1-olefin. Thorough $^{13}C$ NMR copolymer characterization and a statistical elaboration of experimental data, that led to copolymer chains generation, were the *red lines* of the whole research.[3,4]

These results are of relevant interest, from both academic and industrial points of view, because of the importance of block copolymers, materials that have indeed large commercial applications, mostly as thermoplastic elastomers and surfactants. The existing routes for the synthesis of block copolymers rely on both step- and chain-polymerizations.[5] The latter ones are traditionally based on a living polymerization reaction, typically promoted by anionic,[6] cationic,[7] or radicalic catalytic systems.[8] Living coordination catalysts are also available for the preparation of olefin-based block copolymers, by applying a sequential comonomer feed[9] or degenerative chain-transfer conditions.[10] As far as non living coordination catalysts are concerned, they were reported to form blocks in a polyolefin homopolymer: a polypropene with stereoblocks and an appreciable amount of fully atactic polymer was prepared by using fluxional metallocenes endowed with an oscillating geometry during chain growth.[11] Block ethene based copolymers were prepared through the so-called "chain shuttling polymerization" process,[12] with a transfer of growing chains between catalysts endowed with different selectivities, namely stereoselectivity[13] or monomer selectivity.[14]

This work explored to the depth the potentialities of a synthetic route based on $C_2$ symmetric metallocenes to obtain *blocky* ethene (E) based copolymers with 4-methyl-1-pentene (Y) as the comonomer. The characteristics of the ensuing E/Y copolymers and the correlation between catalyst features, such as enantioselectivity and steric hindrance, and copolymer microstructure were investigated.

First, thermal and structural features of *blocky* E/Y copolymers from **EBTHI** (Chart 1), with relatively long sequences of both comonomers able to crystallize were studied, with a particular attention for samples containing a comparable amount of the two comonomers, to investigate the simultaneous presence of crystals arising from homosequences of the two different comonomers. Copolymers homogeneity was analyzed through gel permeation chromatography (GPC) and solvent fractionation. The presence of microcrystalline domains, assessed by means of differential scanning calorimetry (DSC), successive self-nucleation and annealing (SSA)[15] thermal fractionation, and wide angle X-ray diffraction (WAXD), was correlated with the chemical nature of the comonomer sequences. This manuscript presents thus a complete characterization of *blocky* ethene/4-methyl-1-pentene copolymers, investigating the ability of the comonomers sequences to simultaneously crystallize. Preliminary data showed the melting of ethene and 4-methyl-1-pentene sequences in copolymers rich in E and Y, respectively.[2b]

Moreover, ethene/4-methyl-1-pentene copolymers in a wide range of chemical composition were also prepared with the most isospecific, $C_2$ symmetric, metallocene so far used for the synthesis of ethene/1-olefin copolymers, with the purpose of obtaining a block E/Y copolymer, with longer crystallizable sequences of both comonomers, whose simultaneous presence could be more easily detected. The $C_2$ symmetric *rac*-dimethylsilylbis(2-methyl-4-phenylindenyl)zirconium dichloride [*rac*-$Me_2Si$(2-Me-4-PhInd)$_2ZrCl_2$] (**MPHI**), Chart 1, able to prepare a polypropene with 99.5% as isotacticity index,[16] was used as the metallocene and micro- and macro-structural characterization of the ensuing copolymers was carried out.

Surprising results are reported in this manuscript, that not only allow a better understanding of the correlation between catalyst features and copolymer characteristics, but also indicate the existence of unexpected degrees of freedom for the ethene/1-olefin copolymerizations promoted by $C_2$ symmetric metallocenes.

## EXPERIMENTAL SECTION

**Materials.** Toluene (Aldrich) was dried by distillation from sodium under nitrogen atmosphere. Methylaluminoxane (MAO) (Witco, 10 wt % solution in toluene) was used after drying under vacuum to remove solvent and unreacted trimethylaluminum (TMA). [*rac*-(EBTHI)$ZrCl_2$] (**EBTHI**) and [*rac*-$Me_2Si$(2-Me-4-PhInd)$_2ZrCl_2$] (**MPHI**) were provided by Basell Poliolefine Italia Srl. Their molecular structure is shown in Chart 1. Nitrogen and ethene were purified by passage through columns of BASF RS-11 (Fluka) and Linde 4 Å molecular sieves.

**Copolymerization.** The synthesis of the ethene/4-methyl-1-pentene (E/Y) copolymers from **EBTHI** here discussed were previously reported.[2] The series of E/Y copolymers from **MPHI**/MAO catalytic system was prepared as reported in the following section.

**Low-Pressure Copolymerizations.** The copolymerizations were typically performed at 45 °C, in a 250 mL glass reactor equipped with a magnetic stirrer. The reactor was fed with

anhydrous toluene, a fixed amount of 4-methyl-1-pentene, and 10 mL of a MAO solution in toluene (6 mmol of MAO). The total amount of toluene and 4-methyl-1-pentene was 100 mL. After thermal equilibration of the reactor system, ethene was continuously added until saturation. Polymerization was started by adding a solution containing 2 $\mu$mol of **MPHI**. The pressure of ethene was kept constant at 1.03 bar for all the experiments. The copolymerization was terminated by adding a small amount of ethanol and dilute hydrochloric acid, and polymers were then precipitated by pouring the whole reaction mixture into an ethanol excess (1.5 L) to which a proper amount of concentrated hydrochloric acid had been previously added. The adopted reaction conditions allowed to have a very low conversion of 4-methyl-1pentene and, as a consequence, an almost constant ethene/4-methyl-1-pentene ratio throughout the whole copolymerization reaction. Copolymers were collected by filtration and dried under vacuum at 70 °C.

**Copolymer Fractionation.** The fractionation of the copolymers was performed by using solvents with increasing solubility power, at their boiling points. In a round-bottomed flask, equipped with a mechanical stirrer, typically 100 mL of a mixture ethyl ether/ethanol 80/20 v/v and 1.0 g of polymer were introduced. The mixture was allowed to reflux for 1 h and then to reach room temperature under stirring. The solution was then separated from the residual solid polymer by centrifugation for 20 min. The soluble polymer fraction was recovered by drying at 40 °C at reduced pressure for about 12 h and weighed. The unsolved fraction was further fractionated by using *n*-hexane, which has a solubility power higher than that of the ethyl ether/ethanol mixture.

**NMR Analysis.** $^{13}$C NMR spectra of the copolymers were recorded in $C_2D_2Cl_4$ at 103 °C on a Bruker Avance-400 spectrometer operating at 100.58 MHz (internal chemical shift reference: 1% hexamethyldisiloxane). Conditions: 10 mm probe; 90° pulse angle; 64K data points; acquisition time 5.56 s; relaxation delay 20 s; 3K−4K transients. Proton broadband decoupling was achieved using bi_waltz16_32 power-gated decoupling.

**Thermal Analysis.** Thermal behavior of the copolymers was investigated by differential scanning calorimetry (DSC). Heating and cooling curves were recorded on a Mettler DSC 821$^e$ calorimeter, under nitrogen. All samples were treated as follows: after destroying the nascent crystallinity at 260 °C, the specimens were cooled down to −100 °C at a cooling rate of 20 °C/min. A second heating run, again at 20 °C/min, was imposed up to 260 °C to acquire information on the melting behavior of these systems.

To better develop crystallinity, successive self-nucleation and annealing (SSA)[15] thermal fractionation was performed in the same Mettler 821$^e$ DSC instrument on selected copolymer samples. In a typical SSA treatment, specimens were first held at 200 °C for 5 min then cooled at 10 °C/min up to a minimum temperature (e.g., 0 °C), related to the starting of the endothermal phenomena in a "normal" DSC heating run. After holding the samples at the minimum temperature for 5 min, they were heated (10 °C/min) up to a selected self-nucleation temperature, $T_S$, located slightly above the end of the melting endotherm. After holding at $T_S$ for 5 min, the samples were cooled again to the minimum temperature. These steps were repeated several times, each time reaching a maximum temperature 10 °C lower than that of the previous cycle, until the whole melting range was covered. Thermal fractionation takes place according to the length of crystallizable sequences and the final melting curve obtained after a SSA procedure shows a sequence of well-separated peaks, each one corresponding to a set of crystallizable sequences sharing the same average length.

**Structural Analysis.** Room temperature wide-angle X-ray diffraction (WAXD) measurements were carried out on melt-crystallized samples by using a Siemens diffractometer model D-500 equipped with a Siemens FK 60−10, 2000 W Cu tube (Cu $K_\alpha$ radiation, = 0.154 nm) in the $2\theta$ range between 5 and 35°. In order to favor the development of crystallinity, the specimens were submitted to the SSA treatment above specified, obviously except for the final melting step.

## RESULTS AND DISCUSSION

**E/Y Copolymers Obtained with [*rac*-(EBTHI)ZrCl$_2$].** As mentioned in the Introduction, this manuscript presents two new aspects of E/Y copolymers from $C_2$ symmetric metallocenes: a complete characterization of *blocky* E/Y copolymers with both types of sequences able to crystallize and the behavior of the most isospecific metallocene so far used for E/Y copolymers preparation. This first part of the manuscript is focused on a series of E/Y copolymers, having a remarkable amount of both comonomers homosequences and an unusually low alternate comonomer distribution, prepared with the prototypical moderately isospecific metallocene *rac*-ethylenebis(tetrahydroindenyl)zirconium dichloride, **EBTHI**, used to prepare the first prevailingly isotactic polypropene (mmmm =91.5%) from a single center catalyst.[17] The behavior of **EBTHI** in ethene/1-olefin copolymerization emphasizes the powerful action exerted by the bulkiness of a branched 1-olefin, such as 4-methyl-1-pentene, on the comonomer distribution along the polymer chain, as shown by the copolymerization statistics. Indeed, **EBTHI** promotes ethene/propene copolymerizations with a relatively low reactivity ratio product ($r_1r_2 = 0.49$),[18] that turns into a quite high value ($r_1r_2 = 4.5$)[2] when Y is used as the comonomer. As commented in the Introduction, this was attributed to the enhancement of the stereospecific ability of the catalytic center, thanks to the cooperation between the intrinsic chirality of the **EBTHI** organometallic complex and the growing chain containing the bulky comonomer. Copolymerization reactions leading to this original copolymer are presented elsewhere.[2] Discussion in the following aims at illustrating how such unique microstructure reflects upon the structuring of the material.

**Macro- and Microstructural Properties of E/Y Copolymers from [*rac*-(EBTHI)ZrCl$_2$].** In Table 1, data arising from macro- and microstructural characterizations are shown. Copolymers are available in a very broad range of chemical composition, from about 1 to about 95%, as Y molar content. The molecular mass distribution (MMD), i.e. the ratio between weight-average ($M_w$) and number-average ($M_n$) molecular mass, of the copolymers was investigated by GPC, whereas the chemical composition distribution (CCD) was determined from solvent fractionation.

GPC analysis provided MMD values close to 2 (Table 1), as should be expected for copolymers from a single center catalytic system prepared in a polymerization bath with a constant chemical composition. CCD of the copolymers was investigated through a fractionation method[19a] based on the use of solvents, pure or in mixture, with different solubility power and with a standard extraction time (see the Experimental Section). Such a fractionation method, which does not work at the thermodynamic equilibrium and takes advantage of the kinetic aspects of copolymer dissolution, was specifically selected with the aim of separating fractions having even very similar chemical compositions.

**Table 1. E/Y Copolymers from EBTHI: Chemical Composition, Molecular Mass and Molecular Mass Distribution, Triad Distribution[a]**

| run | $f^b$ (mol/mol) | Y[c] (mol %) | $M_w$[d] ($10^{-3}$ g/mol) | MMD[d] | YYY | YYE | EYE | YEY | EEY | EEE |
|---|---|---|---|---|---|---|---|---|---|---|
| 1 | 1.885[e] | 0.95 | 116 | 2.2 | 0.00 | 0.00 | 0.95 | 0.00 | 1.80 | 97.25 |
| 2 | 0.934[e] | 2.16 | 135 | 2.1 | 0.60 | 0.00 | 1.56 | 0.00 | 2.98 | 94.86 |
| 3 | 0.470[e] | 5.22 | 71 | 2.0 | 1.28 | 1.21 | 2.72 | 1.09 | 4.64 | 89.06 |
| 4 | **0**.111[e] | 10.85 | 24 | 2.2 | 1.67 | 2.96 | 6.22 | 2.60 | 10.69 | 75.86 |
| 5 | 0.094 | 18.44 | 8 | 1.7 | 4.97 | 5.93 | 7.54 | 5.85 | 12.51 | 63.19 |
| 6 | 0.060 | 29.66 | 21 | 2.0 | 11.22 | 9.62 | 8.85 | 7.31 | 14.09 | 48.93 |
| 7 | 0.035 | 45.78 | 10 | 1.8 | 23.48 | 13.39 | 8.91 | 10.63 | 11.90 | 31.68 |
| 8 | 0.025 | 54.35 | 13 | 1.8 | 30.89 | 16.08 | 7.38 | 9.74 | 9.63 | 26.28 |
| 9 | 0.024 | 59.92 | 19 | 1.9 | 36.90 | 14.98 | 8.04 | 10.71 | 9.50 | 19.87 |
| 10 | 0.022 | 63.88 | 15 | 1.9 | 41.03 | 16.10 | 6.74 | 11.56 | 8.00 | 16.56 |
| 11 | 0.019 | 69.82 | 24 | 2.3 | 43.27 | 18.69 | 6.49 | 14.36 | 6.36 | 10.83 |
| 12 | 0.010 | 84.56 | 12 | 1.8 | 67.41 | 14.11 | 3.04 | 8.56 | 2.83 | 4.06 |
| 13 | 0.005 | 94.36 | 18 | 2.0 | 81.33 | 11.49 | 1.55 | 4.68 | 0.00 | 0.96 |

[a] Polymerization conditions: total volume =100 mL, [catalyst] = 2 $\mu$mol, Al/Zr = 3000 (mol/mol), $T$ = 45 °C, $P$ = 1.03 bar. Polymerization conditions: total volume =100 mL, [catalyst] = 3 ÷ 10 $\mu$mol, Al/Mt = 1000 (mol/mol), $T$ = 45 °C, $P$ = 2.5 bar. [b] E/Y feed ratio (mol/mol) in liquid phase. [c] From $^{13}$C NMR analysis. [d] Molecular weight and molecular mass distribution from GPC analysis. [e] Reference 2a.

**Table 2. Solvent Fractionation**

| run | fraction no. | solvent(s) and relative amounts | fraction (wt %) | Y[a] (mol %) | $r_1r_2$ |
|---|---|---|---|---|---|
| 5 | raw polymer | | | 18.44 | 5.25 |
| | 1 | ethyl ether/ethanol =80/20 | 61 | 21.53 | 3.80 |
| | 2 | *n*-hexane | 39 | 15.25 | 4.25 |
| | residue | | 0 | - | - |
| 12 | raw polymer | | | 84.56 | 4.30 |
| | 1 | ethyl ether/ethanol =80/20 | 72 | 82.91 | 3.27 |
| | 2 | *n*-hexane | 28 | 87.46 | 8.00 |
| | residue | | 0 | - | - |

[a] From $^{13}$C NMR analysis.

In previous fractionations performed by applying this method,[2a,19] it was shown that it was possible to separate fractions having very close chemical composition and intramolecular comonomer distribution ($r_1r_2$ values).

In Table 2 fractionation data for two copolymers (runs 5 and 12, Table 1) having very different chemical composition are shown.

The fractions obtained from each copolymer exhibit very similar chemical compositions. Moreover, the ethyl ether/ethanol insoluble fractions are fully soluble in boiling *n*-hexane, thus demonstrating that traces of either E or Y homopolymers are not formed under the adopted copolymerization conditions. All the samples with Y ranging from 30 to 70 mol % were treated with boiling ethyl ether and they were found to be completely soluble. The values of $r_1r_2$ products are clearly higher than 1, revealing the blockiness of any copolymer fraction.

These experimental evidence demonstrate that the adopted experimental approach is suitable to prepare copolymers with a narrow intermolecular distribution of molecular properties and allows to assume that the characterization data, namely the $^{13}$C NMR data, are representative of the polymer microstructure and are not simply the average of a blend of copolymer chains.

Triad distributions collected in Table 1, derived from $^{13}$C NMR spectra, indicate that E/Y copolymers from **EBTHI** are characterized by relatively long homosequences of both comonomers, with only a minor presence of alternate comonomer units. In fact, Y homotriad signal was detected even for a copolymer having only 2.1 as mol % of the 1-olefin and the E homotriads were present in all of the investigated copolymers. The sum of the Y and E homotriads was found to be greater than at least 54% (run 11 in Table 1). A comparative analysis of the relative abundance of E rich and Y rich triads leads to the following comments: (i) the EEE/E ratio appears to be higher than the YYY/Y one: for example, run 11 with 69.8 mol % as Y content has a YYY content of 43.3%, whereas run 6 with 70.3 mol % of E has a EEE content of 48.9%; (ii) as far as the alternate triads are concerned, it is worth mentioning that for samples with Y content of at least about 50% by moles (runs 7−13 in Table 1) the amount of YEY triad is higher than that of EYE triad; (iii) taking again into consideration runs 11 and 6, it appears from Table 1 that YEY triad is 14.4% in run 11 while EYE triad is 8.9% in run 6.

A clear picture of the copolymer microstructure appears thus from the copolymer triad distribution. As mentioned above, both the comonomers tend to preferentially form homosequences and, in the case of Y, the homosequences are, to a minor extent, interrupted by single ethene units.

**Statistical Approach.** Copolymerization data were elaborated with a statistical model, the 2nd order Markov model, able to discriminate the influence of both ultimate and penultimate inserted comonomer units.[20] In Table 3, the obtained reactivity

ratios $r_{ij}$, as well as the Comonomer Distribution Index (CDI = $(r_{11}{}^2 r_{22}{}^2 r_{12} r_{21})^{1/3}$), are reported.[2] The CDI value derived from a 2nd order Markov model corresponds to the product of reactivity ratios $r_1 r_2$ obtained from a 1st order Markov model and provides information on the comonomer distribution along the polymer chain.[19c] CDI values greater than 1 indicate the presence of relatively long sequences of both comonomers.

A remarkably high $r_{11}$ value is shown in Table 3, in agreement with the presence of long ethene sequences. Moreover, as already commented,[2] the sequence $r_{11} > r_{21} > 1/r_{12} > 1/r_{22}$ indicates that the E/Y relative reactivity decreases when a Y comonomer is inserted as one or both of the two last inserted comonomer units, confirming the tendency of the catalytic system to form not only ethene (high $r_{11}$ value) but also 1-olefin sequences. The CDI value derived from these reactivity ratios is thus, as expected, larger than 1 and reveals the *blocky* nature of the investigated copolymers.

To provide a sort of fingerprint of the microstructure of such copolymers, the probabilities of having sequences composed of n E units, $[Y(E)_nY]$, or of $n$Y units, $[E(Y)_nE]$, were calculated for run 8 in Table 1 (Y = 54.4 mol %) (see Supporting Information for the calculation method). The calculations were performed using the experimental values of reactivity ratios ($r_{11}$, $r_{12}$, $r_{21}$, and $r_{22}$) given in Table 3, for bath composition $f$ = 0.025. The resulting bar chart is shown in Figure 1.

Both comonomers are prevailingly present along the polymer chain either as isolated units ($n = 1$) or in sequences of more than 12 units. The amount of isolated E units $[Y(E)_1Y]$ is higher than 25% while, on the other hand, more than 85% of the total amount of Y gives rise to homosequences. The almost even distribution of homosequences with n spanning from 2 to 11 really appears as a fingerprint of E/Y copolymers prepared with an isospecific single center catalytic system. The simultaneous presence of sequences of both comonomers that, in principle, should be able to crystallize ($n > 12$)[21] is an intriguing feature of this copolymer that was further investigated in this work. Indeed, it is known that the minimum crystallizable sequence length for linear low density polyethene copolymers range from 8 to about 16 ethene units, depending on crystallization conditions.[21]

**Table 3. Reactivity Ratios for E/Y Copolymerizations from EBTHI**

| $r_{11}$ | $r_{22}$ | $r_{21}$ | $r_{12}$ | CDI | ref |
|---|---|---|---|---|---|
| 134.1 ± 13.7 | 0.09 ± 0.01 | 19.6 ± 3.7 | 0.03 ± 0.01 | 4.5 ± 1.2 | 2a |

**Solid State Properties of E/Y Copolymers from [*rac*-(EBTHI)$ZrCl_2$].** Solid state properties of the E/Y copolymers with the above-described peculiar microstructure were investigated through thermal and structural characterization.

*Thermal Characterization.* The thermal behavior of the copolymers listed in Table 1, as well as that of the two reference homopolymers, was first investigated by traditional DSC analysis. The values of glass transition, crystallization and melting temperatures ($T_g$, $T_c$, and $T_m$, respectively) as well as of the corresponding crystallization and melting enthalpies ($\Delta H_c$ and $\Delta H_m$) are reported in Table 4 for all the samples.

As expected, the glass transition temperature of the copolymers increases with the Y content. The actual $T_g$ values are appreciably higher than those predicted by the Fox−Flory equation for random copolymers; this is likely due to the presence of ordered nanodomains, formed by the longer sequences of ethene units, which result in an amorphous matrix richer in the high $T_g$ component.

In Figure 2, the melting enthalpy values recorded during the second heating run are plotted as a function of copolymer composition. In line with the classical behavior of crystallizable random copolymers, the presence of small amounts of counits has a large impact on melting enthalpy of E/Y copolymers, at both ends of the composition range. This is particularly evident for copolymers with a small Y content, as the polyethene crystalline lattice cannot accommodate the highly hindered Y counits. On the other hand, for Y rich copolymers, the tetragonal form I, typical of melt crystallized isotactic poly(4-methyl-1-pentene),[22] can, at least to some extent, host ethene counits with minor lattice distortion and without paying a large enthalpy penalty.

As already commented, the $r_{ij}$ reactivity ratios shown in Table 3 indicate that the insertion of Y as one or both of the two last inserted comonomer units, in particular as the penultimate inserted unit, remarkably increases the probability of a further Y insertion. It is thus obvious that an increase of Y concentration in the polymerization bath increases the probability for the formation of Y rich sequences and of E sequences with a very minor number of Y units. For example, in the case of the copolymer with 55 mol % of Y, it has been evaluated that around 15 mol % of E and ca. 20 mol % of Y are engaged in the formation

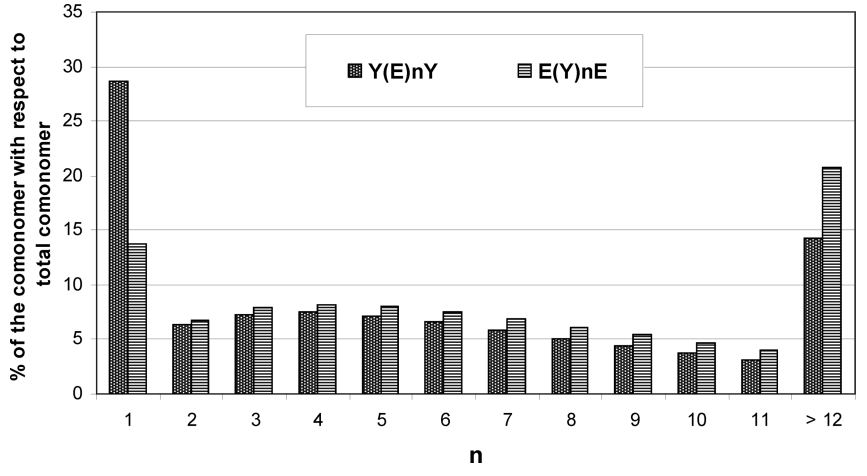


**Figure 1.** Probabilities of sequences of $n$ comonomer units for run 8 in Table 1 (Y = 54.4 mol %).

**Table 4. Thermal Characterization of E/Y Copolymers and of the Reference Homopolymers**

| run | Y (mol %) | $T_g$[a] (°C) | $T_m$[a] (°C) | $\Delta H_m$[a] (J/g) | $T_c$ (°C) | $\Delta H_c$ (J/g) |
|---|---|---|---|---|---|---|
| PE | 0 | n.d.[b] | 140 | 222 | 112 | 219 |
| 1 | 0.95 | n.d.[b] | 126 | 131 | 104 | 133 |
| 2 | 2.16 | n.d.[b] | 118 | 116 | 103 | 118 |
| 3 | 5.22 | n.d.[b] | 114 | 104 | 99 | 103 |
| 4 | 10.85 | n.d.[b] | 89 | 72 | 74 | 70 |
| 5 | 18.44 | −51 | 60[c] | 60 | 40[c] | 60 |
| 6 | 29.66 | −42 | 40[c] | 23 | 12[c] | 23 |
| 7 | 45.78 | −34 | 18 | 1 | 3[d] | 1[d] |
| 8 | 54.35 | −23 | - | - | - | - |
| 9 | 59.92 | −18 | - | - | - | - |
| 10 | 63.88 | −14 | - | - | - | - |
| 11 | 69.82 | −8 | 100 | 2 | - | - |
| 12 | 84.56 | −3 | 154 | 13 | 139 | 12 |
| 13 | 94.36 | 6 | 182 | 29 | 164 | 28 |
| PY | 100 | 26 | 208 | 49 | 191 | 49 |

[a] Measured on 2nd heating. [b] Not detectable. [c] Broad peak. [d] Cold crystallization on 2nd heating.

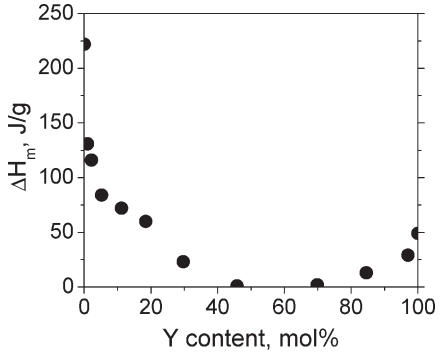


**Figure 2.** Melting enthalpy of melt crystallized E/Y copolymers vs Y molar content..

of homosequences containing at least 12 units (see Figure 1). As already mentioned, the minimum length of a crystallizable ethene sequence is in the range between 8 and 16 ethene units.[21] Therefore, even close to equimolar composition, both the E and Y homosequences can be long enough to crystallize, provided that suitable conditions are met. Actually, upon cooling (at 20 °C/min) from the melt, the copolymers in the composition range between 45 and 70 mol % of Y practically do not show any appreciable endothermic signal. Instead, in the same composition range, two small peaks characterize the DSC trace of as-polymerized samples, isolated by the precipitation from polymer solution. As shown in Figure 3, the two endotherms, which are centered at about 50 and 80 °C have comparable and low intensities (ca. 5 J/g each), and could be assigned to melting of crystals formed by short E and Y sequences, respectively.

*Thermal Fractionation through SSA.* Thermal fractionations based on the use of DSC are powerful methods to "fractionate" polymers from the melt according to the crystallizability of chain segments. In particular, the successive self-nucleation and annealing (SSA) technique, which is based on sequential application of self-nucleation and annealing steps, results in a final melting curve composed of a series of well separated endotherms,

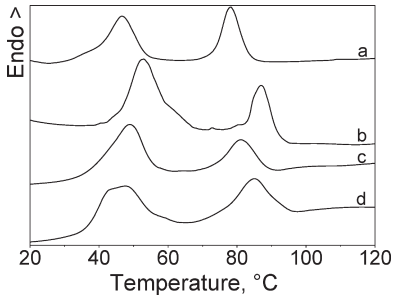


**Figure 3.** DSC heating curves of as-polymerized copolymers. The mol % of Y are as follows: (a) 45.8; (b) 54.3; (c) 59.9; (d) 63.9.

each one corresponding to a set of crystallizable chain sequences sharing the same average length.[15] SSA and, in general, thermal fractionation techniques were applied to provide valuable information on the amount and distribution of short chain branches interrupting the crystallizable polyethene homosequences in ethene/1-olefin copolymers, with 1-olefins varying from C4 to C26.[15,23] A recent work reports on the fractionation by a combination of dissolution/precipitation and temperature gradient extraction of an ethene/propene copolymer synthesized with a Ziegler−Natta catalyst,[24] i.e., a copolymer in which each comonomer unit can, to some extent, be hosted in the crystal lattice of the other comonomer.[25] In fact, after multistep crystallization, single fractions containing relatively long sequences of ethene and propene exhibit WAXD spectra in which the reflections characteristic of the orthorhombic polyethene crystals are present together with those of the α- and γ-polypropene.[24]

The presence of microcrystalline domains in our systems, in particular for the copolymers in the range of equimolar composition, was carefully investigated by means of SSA. The final melting curves resulting from SSA fractionation of a series of selected E/Y copolymers are shown in Figure 4. The broad melting endotherms obtained by classical DSC analysis are replaced by a series of narrow peaks corresponding to the melting of crystallizable sequences of different length.

It is worth noting that at any composition, including those in the equimolar range, endothermic signals corresponding to melting of crystals with a variety of compositional and morphological features appear in the final DSC trace. Taking into account the temperature ranges in which the multiple endotherms appear for the different compositions, it can be reasonably assumed that these peaks correspond to melting of either E or Y short sequences. Moving from DSC traces *a* and *i*, relating, respectively, to copolymers with the highest E and Y content, toward DSC traces *e* and *f*, corresponding to copolymers with nearly equimolar composition, it can be observed a clear decrease of the overall crystallinity and a gradual shift of the melting range to lower temperatures. This is a straightforward consequence of the shortening of both types of homosequences, which reflects upon the formation of progressively thinner lamellae. A close look at *e* and *f* curves, corresponding to copolymers with ca. equimolar composition, shows evidence of endothermic effects in two temperature ranges: one above 50 °C, and the other extending to subambient temperatures. In the light of the other traces reported in Figure 4 and in particular of the above commented shift to lower temperature of melting ranges, endotherms above 50 °C could be assigned to melting of Y crystals, whereas endotherms extending to subambient temperatures could correspond to melting of crystals formed by short E sequences.

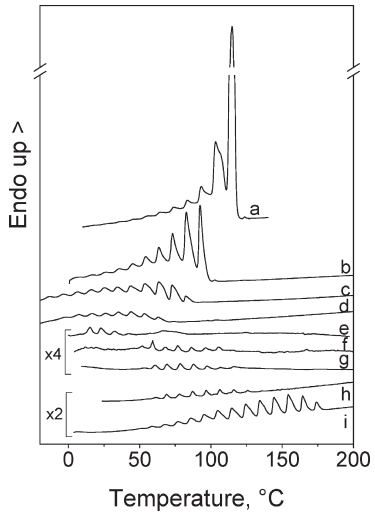


**Figure 4.** Final melting curves obtained after SSA thermal fractionation of E/Y copolymers at increasing Y content. The compositions expressed in 4-methyl-1-pentene mol % are as follows: (a) 5.2; (b) 10.8; (c) 18.4; (d) 29.7; (e) 45.8; (f) 54.3; (g) 59.9; (h) 69.8; (i) 84.6. The curves are shifted vertically for sake of clarity.

Traces *e* − *g* in Figure 4 refer to samples whose DSC first heating curves are shown in Figure 3 (traces a−c). It seems possible to observe, in particular for trace *e* of Figure 4, corresponding to run 7 of Table 1, the contemporary presence of small endotherms in the two mentioned temperature ranges, leading thus to hypothesize the simultaneous existence of crystals due to the two different comonomers, as already done observing the corresponding trace *a* in Figure 3. However, it has to be born in mind that, for compositions approaching the equimolar one, the overall melting enthalpy related to the series of endotherms at low temperatures, likely pertaining to polyethene crystals, is in the order of a few J/g, thus indicating that only a fraction of the E sequences forms thin and defective crystals, difficult to be detected.

**X-ray Diffraction Characterization.** WAXD patterns were collected at room temperature from copolymer samples submitted to the same SSA thermal treatment except the final heating run. They are shown in Figure 5, in which the diffractograms acquired on specimens of the two homopolymers after direct melt crystallization are also reported as references. Reflections at $2\theta$ equal to 21.5° and 24.0°, typical of orthorhombic polyethene crystals,[26] are detectable in copolymer samples containing up to 20 mol % of Y (trace c). The constant value of the Bragg spacing confirms that Y does not enter in the polyethene crystal lattice. In fact, in this case, reflections of pseudohexagonal cell should be observed.[27] In spite of the evidence of crystallinity acquired by DSC in the copolymer with 29.7 mol % of Y, the corresponding WAXD pattern (not shown) does not reveal any discrete reflection, likely as a consequence of the small size of the crystallites and of the fact that part of them melt at subambient temperatures.

Isotactic poly(4-methyl-1-pentene) is known to give rise to a rich polymorphism: five different structures are reported in the literature, depending on crystallization conditions, e.g., from solutions in different solvents or from the molten state after different thermal, pressure or stress histories.[22] The tetragonal form I is the most stable polymorph and is directly obtained by cooling from the molten state.[28] In Figure 5, the reflections

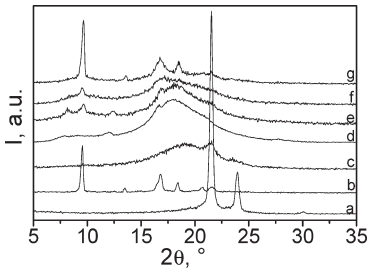


**Figure 5.** WAXD patterns of a selection of E/Y copolymers: (a) polyethene and (b) poly(4-methyl-1-pentene) homopolymers. The mol % of Y are as follows: (c) 18.4; (d) 45.8; (e) 54.4; (f) 69.8; (g) 84.6. The curves are shifted vertically for sake of clarity.

featuring this polymorph, at $2\theta$ = 9.80, 16.50, and 18.35°, are present in the WAXD pattern of the homopolymer as well as of the copolymer containing ca. 15 mol % of ethene: see traces *b* and *g*, respectively. Reflections of form I are also present in the sample containing ca. 30 mol % of ethene units, the peak at $2\theta$ = 9.80°, which corresponds to the (007) plane, being the only one clearly distinguishable in trace *f*. Beside this reflection, two other peaks at $2\theta$ = 8.05 and 12.25° emerge from the broad amorphous halo in trace *e*, which refers to the copolymer with about 55 mol % of Y. According to literature, these new reflections are indicative of the presence of crystals in the hexagonal modification (form IV) which was reported to develop under pressure,[29] and from cyclopentane solutions.[30] We suggest that increasing amount of ethene units in the copolymers favors the formation of this polymorph, either by acting as "*solvent molecules*" for the Y blocks or, by shortening the length of isotactic sequences,[31] in analogy with the role of defective units in the development of α and γ polymorphs of isotactic polypropene. For the copolymer containing about 45 mol % of Y only reflections typical of form IV are detectable in the WAXD spectrum (trace *d*). The occurrence of detectable crystalline reflections of Y crystals even in this sample, which according to the statistical calculations contains no more than 10% of relatively long Y sequences, is likely due to the inclusion in the crystal lattice of isolated ethene units, thus increasing the number and the length of actually crystallizable sequences.

The very low melting point of thin polyethene crystals formed in the final steps of the SSA fractionation would necessitate to acquire WAXD signals under conditions in practice identical to those used with DSC. This would require to perform the SSA treatment in a temperature controlled environment, directly under the X-ray beam, i.e., through an experimental apparatus not available for this work. It was thus not possible to provide undisputable WAXD evidence for the contemporary presence of crystallites formed of homosequences of both components.

The comparative analysis of results from DSC, SSA, and WAXD characterization allows to assume, albeit not to clearly assess, the contemporary presence of small and defective crystallites formed of homosequences of both comonomers. A *blocky* E/Y copolymer with longer comonomer sequences could be thus required to clearly demonstrate that it is possible to obtain simultaneous crystallinities from two comonomer sequences molecularly connected in the same copolymer chain.

**E/Y Copolymers Obtained with *rac*-$Me_2Si$(2-Me-4-PhInd)$_2$ $ZrCl_2$/MAO.** The second part of this work had exactly the objective to prepare a real block ethene/4-methyl-1-pentene copolymer, by using the most isospecific $C_2$ symmetric metallocene so far used

Table 5. $^{13}$C NMR Characterization of E/Y Copolymers from MPHI[a]

| run | $f^b$ (mol/mol) | Y[c] (mol %) | YYY | YYE | EYE | YEY | YEE | EEE | YY | YE | EE |
|---|---|---|---|---|---|---|---|---|---|---|---|
| 14 | 0.658 | 15.04 | 1.57 | 5.23 | 8.24 | 6.48 | 11.54 | 66.94 | 3.70 | 21.75 | 74.56 |
| 15 | 0.372 | 37.62 | 8.39 | 16.52 | 12.72 | 11.56 | 12.08 | 38.73 | 17.38 | 37.44 | 45.18 |
| 16 | 0.288 | 46.20 | 12.00 | 21.14 | 13.06 | 14.52 | 13.05 | 26.24 | 25.51 | 42.81 | 31.69 |
| 17 | 0.259 | 50.64 | 11.27 | 23.65 | 15.72 | 16.06 | 16.67 | 16.63 | 20.52 | 56.55 | 22.92 |
| 18 | 0.149 | 66.81 | 20.60 | 32.58 | 13.62 | 17.14 | 8.12 | 7.93 | 42.45 | 47.37 | 10.18 |

[a] Polymerization conditions: total volume = 100 mL, [catalyst] = 2 $\mu$mol, Al/Zr = 3000 (mol/mol), $T$ = 45 °C, $P$ = 1.03 bar. [b] E/Y feed ratio (mol/mol) in liquid phase. [c] From triad distribution as Y = (YYY + YYE + EYE).

Table 6. Polypropene Isotacticity Index (I.I.), $R$ and $r_{ij}$ Reactivity Ratios, and CDI Values in E/Y Copolymerizations for EBTHI, TBI, and MPHI as the Catalysts Precursors

| | I.I. (mmmm %) | $R^a$ | $r_{11}$ | $r_{21}$ | $r_{12}$ | $r_{22}$ | CDI |
|---|---|---|---|---|---|---|---|
| **EBTHI** | 91.5 | 36.7 | 134.1 ± 13.7 | 19.6 ± 3.7 | 0.029 ± 0.006 | 0.094 ± 0.008 | 4.5 ± 1.2 |
| **TBI**[b] | 97.0 | 28.7 | 109.7 ± 25.4 | 7.0 ± 3.0 | 0.116 ± 0.064 | 0.096 ± 0.013 | 4.5 ± 2.6 |
| **MPHI** | 99.5 | 4.5 | 14.3 ± 2.3 | 1.4 ± 0.3 | 0.23 ± 0.05 | 0.22 ± 0.04 | 1.5 ± 0.6 |

[a] R = (E/Y) copolymer/(E/Y) feed. [b] Reference 2a.

for E/Y synthesis: *rac*-$Me_2Si(2\text{-}Me\text{-}4\text{-}PhInd)_2ZrCl_2$, that was reported to prepare a polypropene with 99.5%[16] as isotacticity index and to promote ethene/propene copolymerizations with a relatively high reactivity ratios product ($r_1r_2$ = 2.1).[18b,32] A more general objective of the research activity here reported was to answer the following questions: what could be the behavior in copolymerization of an isospecific catalyst and the consequent copolymer features, when the catalyst enantioselectivity comes close to perfection?

**Synthesis and Microstructural Characterization of Copolymers from *rac*-$Me_2Si(2\text{-}Me\text{-}4\text{-}PhInd)_2ZrCl_2$/MAO.** Copolymerization reactions were carried out as explained in the experimental part, in the frame of experimental conditions discussed in previous publications:[2] a series of E/Y copolymers was prepared in a wide range of chemical composition, from about 15 to about 67% as Y molar content. Results arising from $^{13}$C NMR microstructural characterization are summarized in Table 5, whereas Table 6 shows the reactivity ratios $r_{ij}$ and the CDI for E/Y copolymers from **MPHI** as well as from **EBTHI**. Data from *rac*-methylene(3-*tert*-butylindenyl)zirconium dichloride, [*rac*-$CH_2(3\text{-}t\text{BuInd})_2ZrCl_2$] catalyst (**TBI**), used in previous works,[2,18c] are reported for comparison.

Data in Table 5 and 6, particularly if considered in a comparative way, are partially in line with what expected but also, to an appreciable extent, surprising. In order to attempt a comprehensive explanation for these findings, it is probably better to start from the results that could have been expected, beginning with the CDI values. In fact, a comparison of CDI values confirms that, in analogy with the other $C_2$ symmetric metallocenes, *rac*-$Me_2Si(2\text{-}Me\text{-}4\text{-}Ph\text{-}Ind)_2ZrCl_2$ gives rise to a CDI higher than 1, i.e. promotes the synthesis of *blocky* E/Y copolymers, even though the 1.5 value appears quite lower than the one (4.5) of the metallocene with the closer isoselectivity, **TBI**. Dwelling upon data of Table 6, it is evident that $r_{ij}$ reactivity ratios of **MPHI** are different from the ones of the other metallocenes, in particular as far as the relative comonomer reactivities, when Y is the last inserted unit, are concerned. In fact, both $r_{12}$ and $r_{22}$ values are higher for **MPHI**, and in the case of $r_{22}$, the value is more than twice. This emphasizes the correlation between isoselectivity of the catalytic center and the easy 1-olefin propagation: the most isospecific metallocene has the highest tendency to insert 4-methyl-1-pentene, as shown by data in Table 6 that indeed show a correlation between $r_{22}$ value and polypropene isotacticity index. Moreover, it is worth observing that, for **MPHI**, the same relative Y/E reactivity ($r_{12} \approx r_{22}$) was determined when either E or Y was the penultimate inserted unit, suggesting that a last inserted Y unit is the key to enhance the Y olefin reactivity. Indeed, from the data of Table 6, it appears that a catalytic center based on a highly isospecific metallocene such as **MPHI** with a bulky 1-olefin as the ultimate inserted unit has a unique behavior: it has not the need of a further bulky olefin in penultimate position to increase the 1-olefin reactivity, as in the case of the moderately isospecific **EBTHI**. However, the effect of a Y unit, in the penultimate position of an E/Y chain growing on **MPHI**, for increasing the Y reactivity, is shown by the lower value of $r_{21}$ with respect to $r_{11}$, even in the presence of a particularly low $r_{11}$ value. The particularly low $r_{11}$, that appears to be responsible of the low CDI, seems also to indicate a low concentration of ethene triads.

Triads distribution from $^{13}$C NMR analysis is the experimental source to derive the reactivity ratios. What commented above should be thus easily demonstrated through the analysis of the triad distribution. Instead, surprisingly, a comparative analysis of triad distributions in E/Y copolymers, prepared with metallocenes whose reactivity ratios are in Table 6, shows that this is not the case, as it can be observed in Figure 6, where the relative concentration of homotriads EEE/E and YYY/Y is plotted versus the 4-methyl-1-pentene content for copolymers from **EBTHI** and **MPHI**.

It is clear that **MPHI** promotes the formation of shorter Y sequences. Data in Table 1 and 5 of this manuscript allow the following quantitative comparison: a sample from **EBTHI** with 69.8 mol % as Y content (run 11 in Table 1) has 43.3 mol % as YYY content, whereas a sample from **MPHI** and with 66.8 mol % as Y content (run 18 in Table 5) has only 20.6 mol % as YYY content.

Moreover, **MPHI** promotes as well the formation of shorter ethene sequences, as demonstrated by the very low $r_{21}$ value, particularly in samples with the larger Y content. Run 11 in Table 1, from **EBTHI** and with 69.8 mol % of Y content, has 10.8 mol % as EEE content, whereas run 18 in Table 5, from **MPHI** and with 66.8 mol % of Y content, has only 7.93 mol % of EEE content.


dx.doi.org/10.1021/ma102914r |*Macromolecules* 2011, 44, 3712–3722

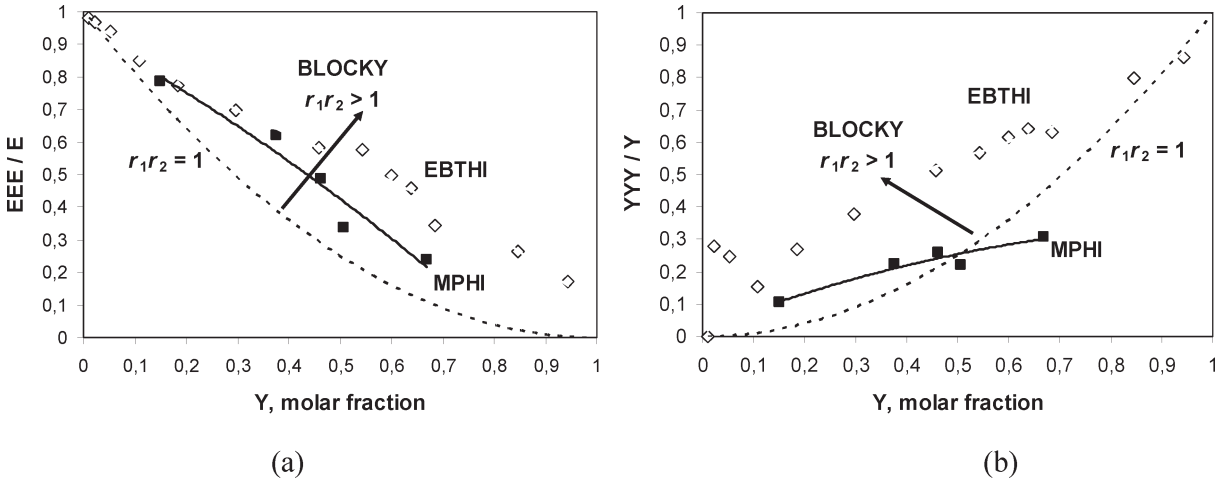


**Figure 6.** Relative concentration of homotriads EEE/E (a) and YYY/Y (b) vs 4-methyl-1-pentene content for E/Y copolymers from **EBTHI** and **MPHI**.

**Table 7. Sequence Average Length for E/Y Copolymers from *rac*-$Me_2Si$(2-Me-4-Ph-Ind)$_2ZrCl_2$**

| run | Y (mol %) | $n$(Y)[a] | $n$(E)[b] |
|---|---|---|---|
| 14 | 15.04 | 1.38 | 6.93 |
| 15 | 37.62 | 1.79 | 3.54 |
| 16 | 46.20 | 1.95 | 2.56 |
| 17 | 50.64 | 1.83 | 2.02 |
| 18 | 66.81 | 2.23 | 1.57 |

[a] $n(Y) = Y/(EYE + 0.5 \cdot YYE)$, where Y = YYY + YYE + EYE. [b] $n(E) = E/(YEY + 0.5 \cdot YEE)$, where E = EEE + EEY + YEY.

The relatively low concentration of E and Y homotriads in the copolymer chain has, as an obvious consequence, the high concentration of heterotriads such as, for example, YYE. For example, run 7 in Table 1, from **EBTHI** and with 45.8 mol % of Y content, has 13.39 mol % of YYE content, whereas run 16 in Table 5, from **MPHI** and with 46.2 mol % of Y content, has 21.14 mol % of YYE content. It is important to underline that, in E/Y copolymers from **MPHI**, Y presents itself in the form of YYE rather than in YYY sequences, whatever the comonomer content is. The particularly slight increase of the average sequences length $n$(Y) on increasing Y content, shown by the data in Table 7, accounts for this observation.

Data so far discussed from **MPHI** seem to present a paradox: the increase of catalyst isoselectivity and reactivity for the 1-olefin causes an easier 1-olefin propagation but, at the same time, shorter 1-olefin sequences. An explanation of these unexpected findings can be proposed by considering the $R$ parameter, that gives the E/Y relative reactivity and it is calculated through the following expression:

$$R = (E/Y)_{copolymer}/(E/Y)_{polymerization\ bath}$$

By examining the $R$ values in Table 6, it is clear that **MPHI** has a particularly low R value. This implies that, to prepare E/Y copolymers with **MPHI**, a relatively low Y concentration has to be used in the polymerization bath. The low Y homotriads content seems thus to be due to a low Y concentration in the polymerization bath and can be justified even in the presence of a high $r_{22}$ value. The high reactivity of **MPHI** for a bulky comonomer such as 4-methyl-1-pentene can be explained with the relatively low steric hindrance of this organometallic complex, definitely lower than the one of **TBI**.

Since the first works on *blocky* ethene/1-olefin copolymers from $C_2$ symmetric metallocenes,[18a] the high isoselectivity and the steric hindrance of the catalyst precursor were indicated as the causes for the formation of *blocky* copolymers. Results reported in this manuscript allow for the first time to tell apart the influence, on the comonomer sequence along a copolymer chain, of high isoselectivity and steric hindrance of the catalyst precursor: the former catalyst feature is the prerequisite for having an easy 1-olefin propagation, whereas the latter one promotes the formation of 1-olefin sequences.

**A Unique Microstructure of E/Y Copolymers from *rac*-$Me_2Si$(2-Me-4-PhInd)$_2ZrCl_2$/MAO.** The detailed comparative analysis proposed in the previous paragraph allows to conclude that the most isospecific **MPHI** metallocene, endowed with a lower steric hindrance, gives rise to a unique behavior in copolymerization and to a unique copolymer microstructure. This latter aspect can be clearly visualized by comparing chain segments, shown in Figure 7, of E/Y copolymers from **EBTHI** and from **MPHI**, obtained through chain generation.[2b,18 d] E/Y copolymers from **MPHI** are characterized by the presence of (very) short E and Y sequences randomly distributed along the polymer chain.

**Thermal Properties of E/Y Copolymers from *rac*-$Me_2Si$(2-Me-4-PhInd)$_2ZrCl_2$/MAO.** The peculiar copolymer microstructure described in the previous paragraph can not but have consequences on the copolymers thermal properties, that were investigated through DSC, by performing a heating−cooling−heating cycle, as for the previous series of investigated copolymers.

Differently from the E/Y copolymer series from **EBTHI**, which showed a certain crystallinity even in proximity of equimolar composition, the copolymers from **MPHI** result to be amorphous in the investigated composition range, as testified by the presence of the only glass transition phenomenon. Glass transition temperatures are reported in Table 8.

While for the copolymer from **EBTHI** containing 46 mol % of Y units melting endotherms were still detectable (see Figures 3 and 4), in the case of **MPHI** catalyst already the copolymer with 15 mol % of Y shows an almost amorphous behavior, more similarly with what expected for random copolymers (A comparison

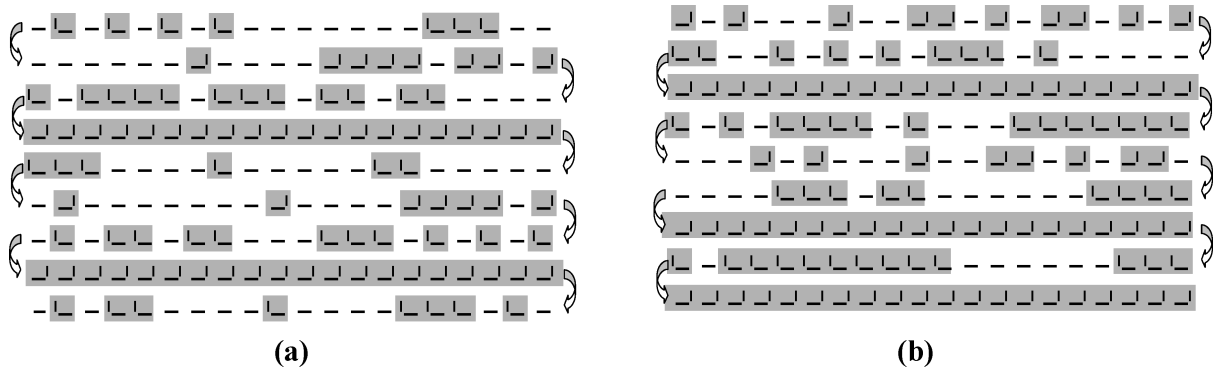


**Figure 7.** Chain segments generated using the Markovian parameters obtained from the reactivity ratios of Table 6 relative to **MPHI** (a) and **EBTHI** (b) metallocene. *f*1/*f*2 ratio was set at 0.224 (**MPHI**) and 0.031 mol/mol (**EBTHI**) to produce a chain with 50/50 comonomer molar ratio. Key: ethene unit, − ; 4-methyl-1-pentene unit, _| (in gray shading)..

**Table 8. Glass Transition Temperatures of E/Y Copolymers from *rac*-$Me_2Si$(2-Me-4-PhInd)$_2ZrCl_2$**

| run | Y (mol %) | $T_g$[a] (°C) |
|---|---|---|
| 14 | 15.04 | −44 |
| 15 | 37.62 | −28 |
| 16 | 46.20 | −26 |
| 17 | 50.64 | −25 |

[a] Measured on 2$^{nd}$ heating.

of the DSC traces of samples from the two catalysts is reported in the Supporting Information).

## CONCLUSIONS

This manuscript was on ethene/4-methyl-1-pentene copolymers from non living $C_2$ symmetric isospecific metallocenes: the moderately isospecific *rac*-ethylenebis(tetrahydroindenyl)zirconium dichloride (**EBTHI**) and the highly isospecific *rac*-dimethylsilylbis(2-methyl-4-phenylindenyl)zirconium dichloride (**MPHI**) being **MPHI** the most isospecific catalyst precursor so far used for the synthesis of E/Y copolymers. Characterization of E/Y copolymers, prepared over a wide range of chemical composition, was performed through $^{13}C$ NMR, determining the comonomer sequences at the triad level, copolymerization reactivity ratios and their products, obtained through a statistical elaboration based on a 2$^{nd}$ order Markov model.

E/Y copolymers from **EBTHI** are essentially made of ethene homosequences alternating with 4-methyl-1-pentene homosequences, with a minor amount of isolated ethene units distributed in the 1-olefin sequence, as shown by the values of $r_{ij}$ reactivity ratios and by the CDI index, clearly higher than 1. The probabilities of sequences composed of n ethene units, $[Y(E)_nY]$, or n 4-methyl-1-pentene units, $[E(Y)_nE]$, were calculated for a copolymer having 54.4 mol % of Y, discovering, for both comonomers, an almost even distribution of homosequences with n spanning from 2 to 11 and the simultaneous presence of sequences with $n > 12$. This suggested the unique possibility that molecularly connected crystals of polyethene and poly(4-methyl-1-pentene) could be contemporarily present in these systems. A thorough thermal and structural characterization of blocky E/Y copolymers was for the first time performed: evidence gathered by combining DSC and WAXD results seem to suggest that, upon appropriate thermal treatment, two populations of thin and defective crystals can be simultaneously present in the copolymers in the range of equimolar composition.

The most isospecific metallocene **MPHI** ever used in E/Y copolymerizations was then adopted with the aim of enhancing the blockiness of the copolymers and investigating what could be the behavior in copolymerization of an isospecific catalyst and the consequent copolymer features, when its enantioselectivity comes close to perfection. **MPHI** revealed the highest tendency ever detected in E/Y copolymerization for the 1-olefin propagation: the highest values for the $r_{12}$ and $r_{22}$ reactivity ratios were in fact calculated, in the presence of the lowest values of $r_{11}$ and $r_{21}$ ratios. A low amount of ethene homotriads, i.e. short ethene sequences, were observed in the copolymer chain, however and surprisingly in the presence of short sequences of 4-methyl-1-pentene as well. Chain generation was performed for copolymers from both **EBTHI** and **MPHI**, revealing, in the latter case, a novel and unique microstructure: very short sequences of both comonomers are almost randomly distributed along the polymer chain. As a consequence of this microstructure, an amorphous nature was revealed for these copolymers by thermal analysis.

Results to E/Y copolymers discussed in this manuscript, arising from a moderately and a highly isospecific metallocene, **EBTHI** and **MPHI** respectively, propose an apparent paradox: the 1-olefin propagation becomes easier by increasing the catalyst isoselectivity but, at the same time, short 1-olefin sequences are formed with the most isospecific metallocene. To solve this apparent contradiction, the lower steric hindrance of **MPHI** was assumed to give rise to a higher reactivity for the 1-olefin and, as a consequence, to a lower concentration of 1-olefin in the polymerization bath and of 1-olefin sequences in the copolymer chain.

In all the papers on *blocky* ethene/1-olefin copolymers it was reported that single center catalysts required to achieve this copolymer microstructure were based on $C_2$ symmetric, stereorigid, sterically hindered and highly isospecific metallocenes. This manuscript demonstrates, for the first time, that it is possible to tell apart the influence of isoselectivity and steric hindrance and shows the existence of unexpected degrees of freedom for tuning microstructure and, in turn, properties of ethene/1-olefin copolymers from $C_2$ symmetric metallocenes.

In a recent review,[33] polymerizations able to control the monomer sequences were proposed as the Holy Grail in polymer science. The author said that tools for controlling polymers microstructures, such as sequences and tacticity, are still rudimentary and that "as learned from nature, sequence-controlled

polymers are most likely the key toward functional sub-nanometric materials". This work is intended to be a contribution in this direction.

## ■ ASSOCIATED CONTENT

**Supporting Information.** Description of the procedure adopted for the calculation of sequence length probability reported in the text and comparison of DSC traces of copolymers from the two catalysts. This material is available free of charge via the Internet at http://pubs.acs.org.

## ■ AUTHOR INFORMATION

### Corresponding Author

*(P.S.) stagnaro@ge.ismac.cnr.it. Telephone: +39 010 6475874. Fax: +39 010 6475880. (S.L.) s.losio@ismac.cnr.it. Telephone: +39 02 23699750. Fax: +39 02 70636400..

## ■ ACKNOWLEDGMENT

This study was supported by Regione Lombardia (Project 4161-MOD-IM-PACK, 2008-2009). The authors thank Dr. Laura Alagia for her valuable contribution in the Experimental Section.

## ■ REFERENCES

(1) Zambelli, A.; Grassi, A.; Galimberti, M.; Mazzocchi, R.; Piemontesi, F. *Makromol. Chem., Rapid Commun.* **1991**, *12*, 523–528.

(2) (a) Galimberti, M.; Piemontesi, F.; Alagia, L.; Losio, S.; Boragno, L.; Stagnaro, P.; Sacchi, M. C. *J. Polym. Sci., Polym. Chem.* **2010**, *48*, 2063–2075. (b) Losio, S.; Stagnaro, P.; Motta, T.; Sacchi, M. C.; Piemontesi, F.; Galimberti, M. *Macromolecules* **2008**, *41*, 1104–1111.

(3) (a) Losio, S.; Tritto, I.; Zannoni, G.; Sacchi, M. C. *Macromolecules* **2006**, *39*, 8920–8927. (b) Losio, S.; Boccia, A. C.; Boggioni, L.; Sacchi, M. C.; Ferro, D. R. *Macromolecules* **2009**, *42*, 6964–6971.

(4) Losio, S.; Boccia, A. C.; Sacchi, M. C. *Macromol. Chem. Phys.* **2008**, *209*, 1115–1128.

(5) Hadjichristidis, N.; Pispas, S.; Floudas, G. A. *Block copolymers. Synthetic strategies, physical properties, and aplications*; Wiley Interscience, John Wiley & Sons: New York, 2003.

(6) Hadjichristidis, N.; Pitsikalis, M.; Pispas, S. *Chem. Rev.* **2001**, *101*, 3747–3792and references therein..

(7) *Cationic polymerization. Mechanisms, synthesis and applications*; Matyjaszewski, K., Ed.; CRC Press: New York, 1996.

(8) Matyjaszewski, K.; Xia, J. *Chem. Rev.* **2001**, *101*, 2921–2990and references therein..

(9) Coates, G. W.; Hustad, P. D.; Reinatz, S. *Angew. Chem., Int. Ed.* **2002**, *41*, 2236–2257and references therein..

(10) (a) Harney, M. B.; Zhang, Y.; Sita, L. R. *Angew. Chem., Int. Ed.* **2006**, *45*, 2400–2404. (b) Harney, M. B.; Zhang, Y.; Sita, L. R. *Angew. Chem., Int. Ed.* **2006**, *45*, 6140–6144.

(11) (a) Coates, G. W.; Waymouth, R. M. *Science* **1995**, *267*, 217–219. (b) Lin, S.; Waymouth, R. M. *Acc. Chem. Res.* **2002**, *35*, 765–773.

(12) (a) Chien, J. C. W.; Iwamoto, Y.; Raush, M. D.; Wedler, W.; Winter, H. H. *Macromolecules* **1997**, *30*, 3447–3458. (b) Chien, J. C. W.; Iwamoto, Y.; Raush, M. D. *J. Polym. Sci., Polym. Chem.* **1999**, *37*, 2439–2445. (c) Lieber, S.; Brintzinger, H. H. *Macromolecules* **2000**, *33*, 9192–9199. (d) Jayaratne, K. C.; Sita, L. R. *J. Am. Chem. Soc.* **2001**, *123*, 10754–10755. (e) Bhriain, N. N.; Brintzinger, H. H.; Rhucatz, D.; Fink, G. *Macromolecules* **2005**, *38*, 2056–2063.

(13) Arriola, D. J.; Carnaham, E. M.; Hustad, P. D.; Kulman, R. L.; Wenzel, T. T. *Science* **2006**, *312*, 714–719and references therein.

(14) Alfano, F.; Boone, H. W.; Busico, V.; Cipullo, R.; Stevens, J. C. *Macromolecules* **2007**, *40*, 7736–7738.

(15) (a) Müller, A. J.; Hernandez, Z. H.; Arnal, M. L.; Sanchez, J. J. *Polym. Bull.* **1997**, *39*, 465–472. (b) Müller, A. J.; Arnal, M. L. *Prog. Polym. Sci.* **2005**, *30*, 559–603. (c) Lorenzo, A. T.; Arnal, M. L.; Müller, A. J.; Boschetti de Fierro, A.; Abetz, V. *Macromol. Chem. Phys.* **2006**, *207*, 39–49.

(16) Resconi, L.; Fait., A.; Piemontesi, F.; Cavallo, G. *Chem. Rev.* **2000**, *100*, 1253–1345.

(17) Kaminsky, W.; Külper, K.; Brintzinger, H. H.; Wild, F. R. W. P. *Angew. Chem. Int. Ed.* **1985**, *24*, 507–508.

(18) (a) Galimberti, M.; Piemontesi, F.; Fusco, O.; Camurati, I.; Destro, M. *Macromolecules* **1998**, *31*, 3409–3416. (b) Galimberti, M.; Piemontesi, F.; Fusco, O.; Camurati, I.; Destro, M. *Macromolecules* **1999**, *32*, 7968–7976. (c) Losio, S.; Piemontesi, F.; Forlini, F.; Sacchi, M. C.; Tritto, I.; Stagnaro, P.; Zecchi, G.; Galimberti, M. *Macromolecules* **2006**, *39*, 8223–8228.

(19) (a) Dall'Occo, T.; Galimberti, M.; Balbontin, G. *Polym. Adv. Technol.* **1992**, *4*, 429–434. (b) Galimberti, M.; Destro, M.; Fusco, O.; Piemontesi, F.; Camurati, I. *Macromolecules* **1999**, *32*, 258–263. (c) Galimberti, M.; Piemontesi, F.; Baruzzi, G.; Mascellani, N.; Camurati, I.; Fusco, O. *Macromol. Chem. Phys.* **2001**, *202*, 2029–2037.

(20) Odian, G. *Principles of Polymerization*, 3rd ed.; Wiley & Sons: NewYork, 1991; pp 503−505.

(21) (a) Luo, H.; Chen, Q.; Yang, G. *Polymer* **2001**, *42*, 8285–8288. (b) Burfield, D. R.; Kashiwa, N. *Makromol. Chem.* **1985**, *186*, 2657–2662. (c) Burfield, D. R. *Macromolecules* **1987**, *20*, 3020–3023.

(22) De Rosa, C. *Macromolecules* **2003**, *36*, 6087–6094and references therein..

(23) (a) Wang, C.; Chu, M.-C.; Lin, T.-L.; Lai, S.-M.; Shih, H.-H.; Yang, J.-C.. *Polymer* **2001**, *42*, 1733–1741. (b) Zhang, F.; Liu, J.; Fu, K.; Huang, H.; Hu, Z.; Yao, S.; Cai, X.; He, T.. *J. Polym. Sci., Part B: Polym. Phys.* **2002**, *40*, 813–821. (c) Piel, C.; Stark, P.; Seppälä, J. V.; Kaminsky, W. *J. Polym. Sci., Part A: Polym. Chem.* **2006**, *44*, 1600–1612.

(24) Dong, Q.; Fan, Z.-H.; Fu, Z.-S.; Xu, J.-T. *J. Appl. Polym. Sci.* **2008**, *107*, 1301–1309.

(25) Alamo, R. G.; Mandelkern, L. *Thermochim. Acta* **1994**, *238*, 155–201.

(26) Bassi, I. W.; Corradini, P.; Fagherazzi, G.; Valvassori, A. *Eur. Polym. J.* **1970**, *6*, 709–718.

(27) Guerra, G.; Galimberti, M.; Piemontesi, F.; Ruiz de Ballesteros, O. *J. Am. Chem. Soc.* **2002**, *124*, 1566–1567.

(28) (a) Natta, G.; Corradini, P.; Bassi, W. *Rend. Fis. Acc. Lincei* **1955**, *19*, 404–411. (b) Frank, F. C.; Keller, A.; O'Connor, A. *Philos. Mag.* **1959**, *8*, 200–214. (c) Bassi, W.; Monsignori, O.; Lorenzi, G. P.; Pino, P.; Corradini, P.; Temussi, P. A. *J. Polym. Sci., Polym. Phys. Ed.* **1971**, *9*, 193–203. (d) Kusanagi, H.; Takase, M.; Chatani, Y.; Takodoro, H. *J. Polym. Sci., Polym. Phys. Ed.* **1978**, *16*, 131–142.

(29) Hasegawa, R.; Tanabe, Y.; Kobayashi, M.; Tadokoro, M.; Sawaoka, A.; Kawai, N. *J. Polym. Sci., Polym. Phys. Ed.* **1970**, *8*, 1073–1087.

(30) Charlet, G.; Delmas, G. *Polym. Bull. (Berlin)* **1982**, *6*, 367–373.

(31) (a) Alamo, R. G.; Ghosal, A.; Chatterjee, J.; Thompson, K. L. *Polymer* **2005**, *46*, 8774–8789. (b) De Rosa, C.; Auriemma, F.; Paolillo, M.; Resconi, L.; Camurati, I. *Macromolecules* **2005**, *38*, 9143–9154. (c) Stagnaro, P.; Costa, G.; Trefiletti, V.; Canetti, M.; Forlini, F.; Alfonso, G. C. *Macromol. Chem. Phys.* **2006**, *207*, 2128–2141.

(32) Busico, V.; Cipullo, R.; Segre, A. L. *Macromol. Chem. Phys.* **2002**, *203*, 1403–1412.

(33) Lutz, J. F. *Polym. Chem.* **2010**, *1*, 55–62.